JOURNAL OF MATERIALS SCIENCE 25 (1990) 3118–3126

Glasses from aerogels

Part 2 The aerogel–glass transformation

T. WOIGNIER, J. PHALIPPOU
Laboratoire de Science des Matériaux Vitreux, Université de Montpellier II, 34060 Montpellier Cédex, France

M. PRASSAS
Corning Europe, Avon, France

Silica glasses are obtained by the densification of aerogels. The transformation of the material into a glass is followed by differential thermal analyis, thermo-gravimetric analysis, dilatometry and by the evolution of the structural, textural and mechanical properties of the material. The organic species and the hydroxyl groups are removed by oxidation and chlorination heat treatments in such a way as to avoid bloating and crystallization phenomena during sintering. Densification is obtained by heat treatment at a low temperature (1100 to 1300° C). The densified aerogel shows physical properties identical to those of molten silica. Moreover, this material is very pure and its water content is low. The same process can be extrapolated to multicomponent glasses and composite materials.

1. Introduction

In Part 1 of this work [1], we have shown that different methods of hypercritical drying are available to synthesize silica aerogels. The main advantage of hypercritical drying concerns the possibility of obtaining dry aerogels which could be transformed into a glass without grinding, compaction or other polluting treatments. However, silica aerogels are amorphous materials, extremely porous and brittle, containing organic and hydroxyl species either as structural or adsorbed groups. During the aerogel–glass conversion, the aerogel must retain its amorphous state. Thermal treatments will be necessary to eliminate the porosity and undesirable chemical species.

The textural, structural characteristics and mechanical properties are strongly dependent on the gelation parameters (pH, temperature, concentration, ageing and also on the hypercritical drying conditions). For example, the bulk density of aerogels can be as low as $0.015\,g\,cm^{-3}$ if the sample is prepared under basic conditions [2] and higher than $0.5\,g\,cm^{-3}$ in acidic catalysis [3]. The mechanical properties can vary between 1 kPa and 1 Mpa for the tensile strength [4] and between 0.1 MPa and 1 GPa for the Young's modulus [1, 3]. Thus, to optimize the sequence of heat treatments leading to silica glass, the aerogel–glass transformation has been studied using a standard aerogel. This material is obtained by the hydrolysis (4 mol H_2O per mol TMOS) of a methanolic solution of tetramethoxysilane (3 volumes of TMOS with 2 volumes of methanol). The alcogel is dried in an autoclave at 270° C and 18 MPa in the presence of an extra volume of methanol [1]. The main characteristics of this aerogel are listed in Table I.

The aerogel–glass transformation will be followed by thermal analysis and by the evolution of the structural, textural and mechanical properties of the material until a "glass-like material", showing physical features identical to those of a conventional silica glass, is obtained.

2. Thermal analysis

Differential thermal analysis (DTA), thermogravimetric analysis (TGA) and dilatometric analysis (DA) cover the three temperature ranges related to the evolution of the aerogel (Fig. 1). In the first temperature range (25 to 250° C) the elimination of adsorbed species (H_2O or organic compounds) is responsible for a low weight loss ($\simeq 0.5\%$) and the observed endothermic DTA peak. The following exothermic events and the associated weight losses ($\simeq 3\%$) are due to the oxidation of the organic species (250 to 500° C) which come from the esterification reaction occurring during the autoclave process.

Between 500 and 1000° C the continuous weight loss is attributed to the condensation of the silanol groups leading to the formation of siloxane bonds. Sintering occurs in this temperature range; it is of a small extent between 500 and 600° C then increases rapidly around 1000° C. The sintering mechanisms will be discussed later.

TABLE I Physical properties of the standard aerogel

Bulk density, ρ_b ($g\,cm^{-3}$)	Skeletal density, ρ_s ($g\,cm^{-3}$)	Pore volume, P_0(%)	Specific surface area, S($m^2\,g^{-1}$)	Young's modulus, E (Pa)	Flexural strength, σ (Pa)	Vickers hardness, H_v ($kg\,mm^{-2}$)
0.3	> 1.85	85	400	1×10^8	5×10^5	$\simeq 1$

0022–2461/90 $03.00 + .12

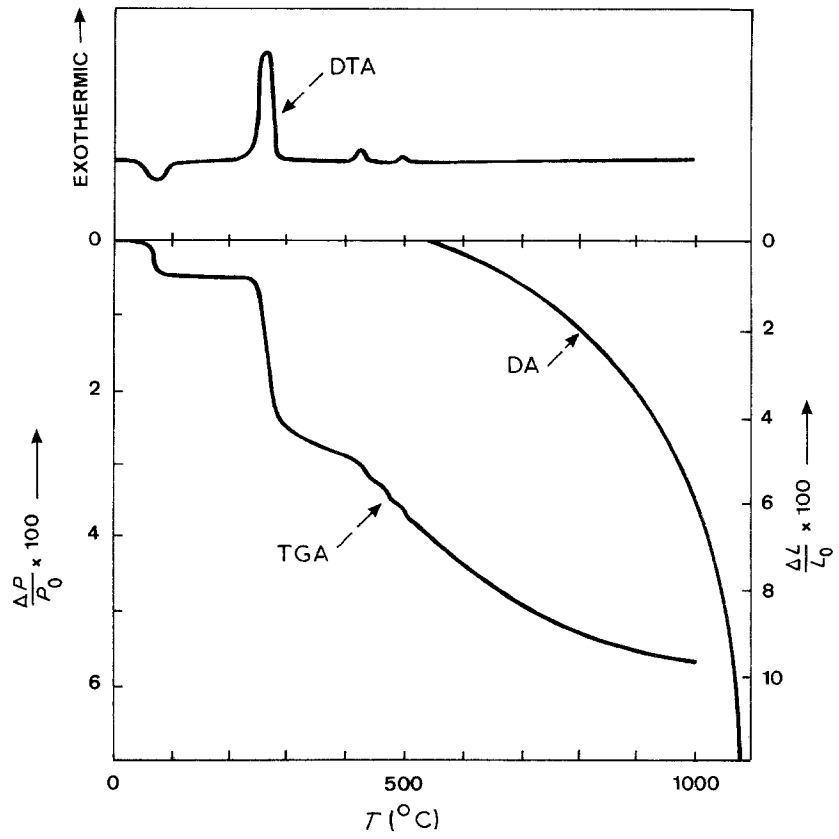

Figure 1 Thermal analysis of the silica aerogel (differential thermal analysis, thermogravimetric analysis, dilatometric analysis).

3. Structural evolution

The structural evolution of the material has been followed by near infrared spectroscopy, 4000 to 10 000 cm^{-1} (Fig. 2). Thin slices of the material (1 mm) are heat treated and studied by transmission spectroscopy at 25° C. The different absorption peaks and their attributions are listed in Table II. They are combinations and harmonics of the fundamental vibration bands observed in the spectral range 1400 to 4000 cm^{-1} [5–7].

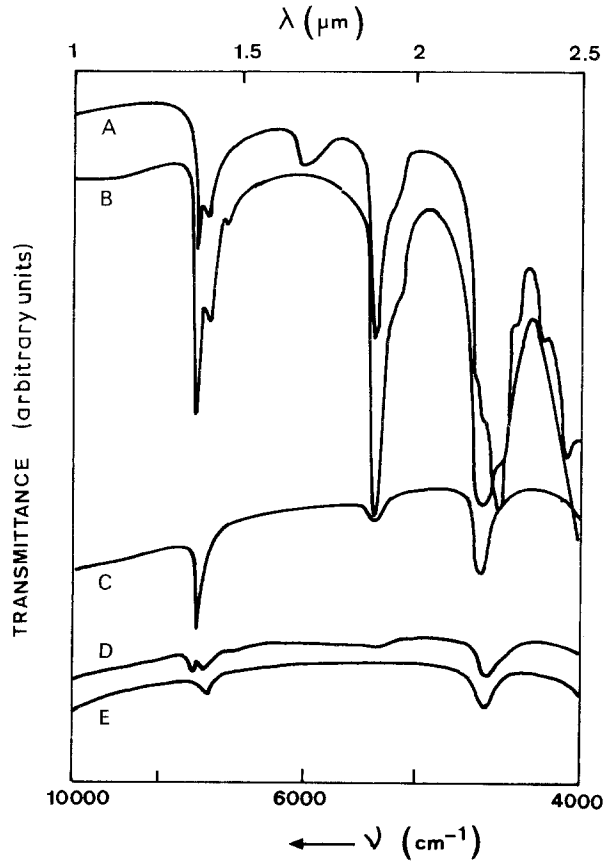

Figure 2 Evolution of the near infrared spectrum of the silica aerogel A (25° C), B (500° C), C (1050° C), D (1130° C), E (1150° C).

After heat treatment at 500° C, the intensity of the peaks attributed to the organic groups decreases. Simultaneously the spectrum shows an increase of the intensity of the silanol and adsorbed water bands. Those phenomena are due to the oxidation of the organic species (observed by TGA and DTA) which transforms the hydrophobic untreated material into a hydrophylic one. Due to a steric effect, the organic species prevent the adsorption of water even if the structure shows the presence of silanol groups. The oxidation heat treatment replaces the organic groups by silanol bonds which are favourite sites for the adsorption of atmospheric moisture during cooling. The appearance of a low peak aroun 6900 cm^{-1} may be due to a combination of the bands at 5230 and 1640 cm^{-1} (H_2O bending).

At 1050° C we observed a decrease in the adsorbed water content. This lower water content is a consequence of the smaller specific surface area exhibited by the material heat treated at 1050° C, as will be seen later.

After heat treatment at 1130° C the spectrum is characteristic of a material intermediate between the gel and the glass. Simultaneously, a peak situated at 7350 cm^{-1} appears, which is due to the free silanols of a porous structure. The band located at 7250 cm^{-1} corresponds to the silanol usually found inside the glass structure. At 1150° C the spectrum is identical to that of a conventional silica glass.

4. Textural evolution

The variation of the textural properties, specific sur-

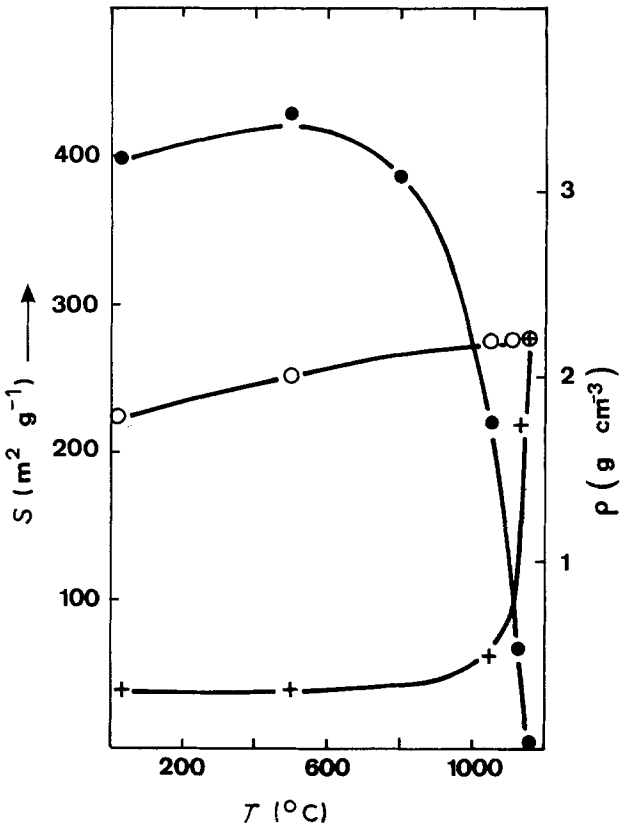

Figure 3 Evolution of (+) the bulk density (ρ_b), (○) skeletal density (ρ_s) and (●) specific surface area (S) as a function of temperature.

face area, S, bulk density, ρ_b, and skeletal density, ρ_s, is shown in Fig. 3. The variation of the bulk density, ρ_b, can be directly related to the dilatometric results: no significant shrinkage is detected below 1000° C for short durations but the sintering becomes rapid in the temperature range 1000 to 1200° C.

A small increase in the specific surface area is observed after oxidation heat treatment. This effect has been attributed to an increase of the macroporosity [9]. In fact it is certainly due to a better accessibility of nitrogen molecules when the steric effect of the organic species present at the surface of the material vanishes. It must be noted that the real specific surface area would be larger than that measured by N_2 BET techniques. Small-angle neutron scattering has indicated a roughness of the particles in the length range 0.3 to 0.8 nm [9] (with a surface fractal dimension close to 3). Specific surface area measured using a nitrogen adsorption isotherm cannot include the surface developed into pores having a radius lower than 0.6 nm.

The skeletal density (or matrix density) is measured by helium pycnometry. For untreated aerogel, the value is close to 1.85 g cm^{-3} [10]. After heat treatments, ρ_s increases up to 2.2 g cm^{-3}. This enhancement can also be attributed to the elimination of the steric effect of the organic species and to the smoothing of the roughness of the particles which occurs during heat treatment [9]. Moreover a slight increase in the skeletal density of aerogel was observed during this thermal treament. An identical phenomenon has been observed in silica xerogel and has been attributed to a structural relaxation [11].

It has been proposed [12, 13] that skeletal density could be as low as 0.5 g cm^{-3}. These values were deduced from small-angle X-ray scattering (SAXS) results and specific surface area measurements and assume that the gel matrix contains a large volume of closed micropores. Our direct measurements obtained using helium pycnometry show clearly that these assumptions are not valid. The matrix of aerogel is formed by a solid phase which is accessible by helium gas; therefore the porosity can be regarded as almost totally open.

5. Evolution of the mechanical properties

The mechanical properties such as Young's modulus (E), mechanical strength (σ) and Vickers hardness (H_v) vary depending on the temperature. At low temperature, before the beginning of sintering, the mechanical properties are not readily modified. However, oxidation heat treatment at 500° C increases the Young's modulus by a factor of two [3]. This increase in the stiffness is related to the formation of new siloxane bonds which replace the organic groups and increase the connectivity of the network. On the other hand, with the oxidation heat treatment, internal silanol groups may also condense to give rise to higher skeletal density. As a consequence the aerogel strengthens.

In fact, the mechanical behaviour of the material is strongly influenced by its bulk density and is related to the sintering temperature range. Fig. 4 shows that E, σ and H_v increase by a factor of 10^3 to 10^4 between the untreated aerogel and the totally densified material. Finally, the mechanical features of the totally densified material are identical to those of conventional silica glass (Table III).

It is noteworthy that evolution of the mechanical properties can be fitted with the following scaling laws

$$E \propto \rho^{3.3}$$

$$\sigma \propto \rho^{2.6}$$

$$H_v \propto \rho^{3.5}$$

TABLE II Absorption bands in the near infrared spectral range

Wave number	Intensity	Assignments
4060	low	Stretching–bending combination modes of hydrogen-bonded silanol groups [5]
4420	strong	Stretching–bending combination modes of C–H bond [7]
4540	low	Stretching–bending combination modes of free silanol groups [5, 6]
5230	strong	Stretching–bending combination modes of molecular water [5, 6]
5700–6000	broad, several peaks	Overtone and combination of asymmetric and symmetric mode of C–H bond [7]
7140	strong	Combination of stretching modes of Si–OH and H–OH bonds
7250	low	Overtone of Si–OH stretching mode (glass structure) [6]
7350	strong	Overtone of Si–OH stretching mode (gel structure)

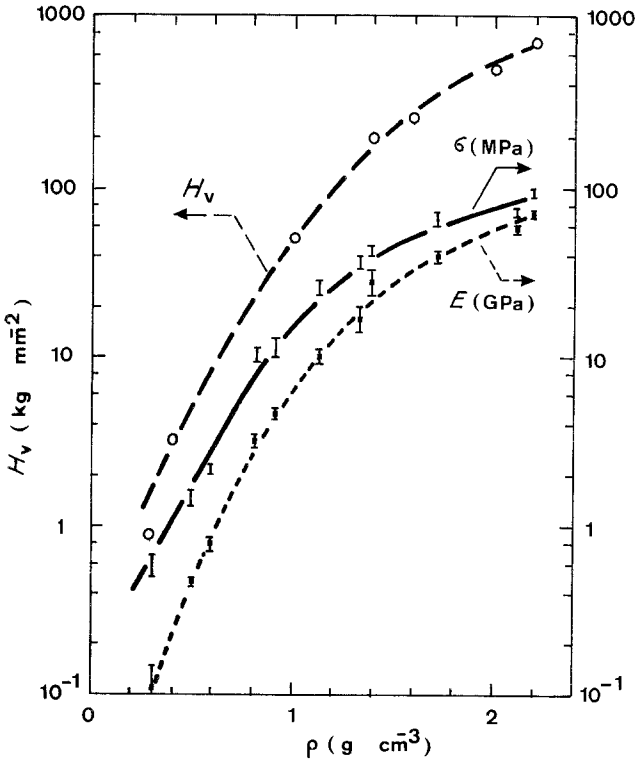

Figure 4 Evolution of the tensile strength (σ), Young's modulus (E) and Vickers hardness (H_v) as a function of the bulk density of the aerogel.

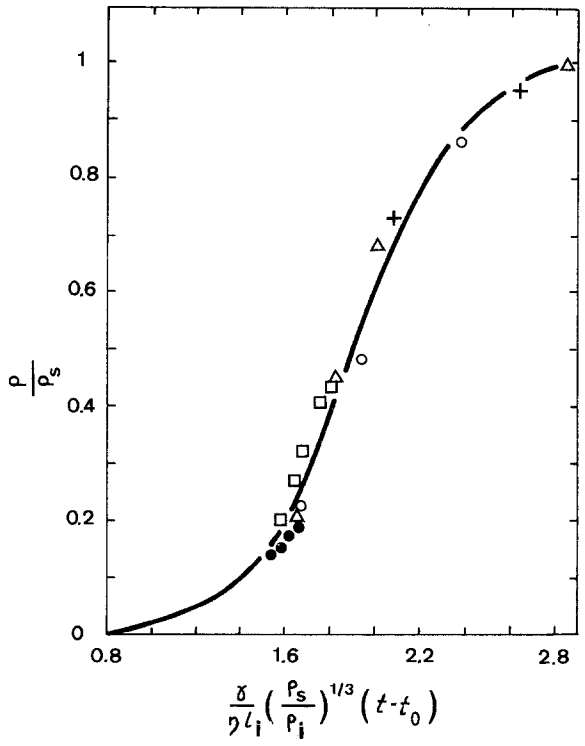

Figure 5 Plot of ρ/ρ_s against $K(t-t_0)$. (——) Fit of experimental sintering to the theoretical curve of the Scherer's model. (●) 1005° C, (□) 1050° C, (△) 1100° C, (○) 1200° C, (+) 1250° C.

and those exponents are not in agreement with the predictions of the classical models used to account for the mechanical properties of cellular materials or expanded foams [14]. On the other hand, it has been claimed that an analogy could exist between a gel network and a percolation cluster [16]. As a consequence, the evolution of mechanical properties of the gels would agree with the predictions of the percolation theory.

In the case of aerogels, we have shown [3, 4] that a percolation theory is not easily applicable due to the absence of a physical parameter clearly related to the percolation probability. Moreover, a percolation cluster has a fractal dimension equal to 2.5 while aerogels show fractal dimensions in the range 1.8 to 2.4. This fractal structure disappears during sintering [2]. Thus the power law dependence of the mechanical properties of aerogels is not related to its fractal structure and is certainly more complex than a straightforward percolation.

6. Sintering mechanism

The identification of the sintering has been obtained by studying the shrinkage kinetics. In a previous work [16], in which the shrinkage was monitored in air and under isothermal conditions, we have shown that two kinds of mechanism are responsible for the sintering. At low temperature the sintering is due to a diffusional process (500 to 700° C); above 1000° C sintering is related to a viscous flow phenomenon with an activation energy of 88 kcal mol^{-1}. In the intermediate temperature range, both processes exist and overlap.

The identification of the viscous flow mechanism and the determination of its activation energy was obtained on the basis of Frenkel's model [17]. However, due to the approximations concerning its geometry, Frenkel's model is not expected to be applicable beyond the early stages of sintering.

To account for the sintering of amorphous materials in a large range of densification, Scherer [18] developed another viscous flow model in which densification results from shrinkage of a cubic array of cylinders. In this model a theoretical curve between the relative density and the reduced time $K(t-t_0)$ is proposed (Fig. 5). t_0 is a fictitious time for which the relative density ρ/ρ_s would be equal to 0, and K is given by

$$K = \frac{\gamma}{\eta l_i}\left(\frac{\rho_s}{\rho_i}\right)^{1/3}$$

where l_i is the initial length of the cubic unit cell, ρ_s the theoretical density and ρ_i the initial density at $t = 0$. γ is the surface energy and η the viscosity.

The large densification of the aerogel is compared with the cylinder model as follows. Samples are isothermally treated at different temperatures in the range 980 to 1250° C. The bulk density is measured as

TABLE III Physical properties of the sintered aerogel

Density, ρ_b (g cm^{-3})	Relative index, nd	Vickers hardness, H_v (kg mm^{-2})	Shear modulus, G (N m^{-2})	Bulk modulus, K (N m^{-2})	Young modulus, E (N m^{-2})	Flexural strength, σ (N m^{-2})
2.2	1.458	750	3.2×10^{10}	3.6×10^{10}	7.3×10^{10}	95×10^{6}

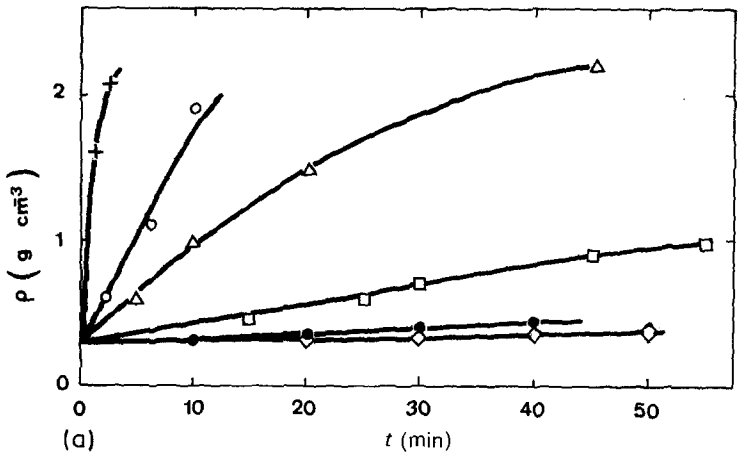

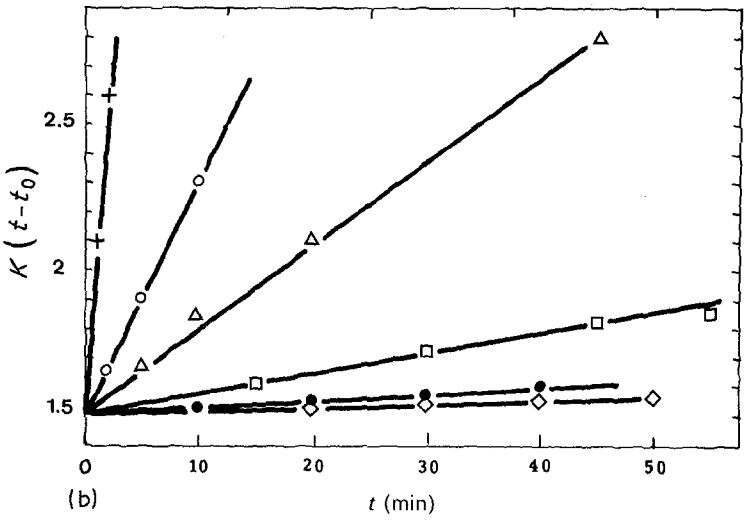

Figure 6 Plots of (a) bulk density and (b) reduced time against sintering time. (◇) 980° C, (●) 1005° C, (□) 1050° C, (△) 1100° C, (○) 1200° C (+) 1250° C.

a function of time (Fig. 6a) and relative density is fitted to the theoretical curve. This procedure allows us to determine the reduced time. If the model applies, the plots of the reduced time as a function of the real time should yield straight lines. The slopes are related to the viscosity at the temperature of interest.

For the aerogel studied, the model works quite well (Figs 5 and 6b). The good quality of the fit to the model shows that the viscosity does not vary during sintering. Thus the hydroxyl content remains constant with time as observed from isothermal T G A measurements. The viscosities are calculated using the surface energy, γ, of the silica (280 erg cm^{-2}) and the l_i value is deduced from the initial relative density and the specific surface area, using the relationship of Scherer's model [19]

$$\frac{\rho_i}{\rho_s} = 3\pi a^2 l_i - 8(2a^3)^{1/2}$$

$$S = \frac{1}{a\rho_s}\left(\frac{6\pi l_i - 24(2a)^{1/2}}{3\pi l_i - 8(2a)^{1/2}}\right)$$

The calculated viscosities are then plotted in Fig. 7 using an Arrhenius-type equation. Viscosity values are found close to those expected in such materials. The activation energy of 82 kcal mol^{-1} agrees well with the previously obtained value (88 kcal mol^{-1}) [16]. Onorato (see [19]) found similar kinetics for densification of aerogels. Moreover the value of viscosity was shown to be dependent on the nature of the atmosphere [19].

In the case of vitreous silica, values ranging from 120 to 170 kcal mol^{-1} were measured when the hydroxyl content varied between 1300 and 3 p.p.m. Our result is in a good agreement with those mentioned above if we consider the high hydroxyl content of our samples. Infrared spectroscopy measurements

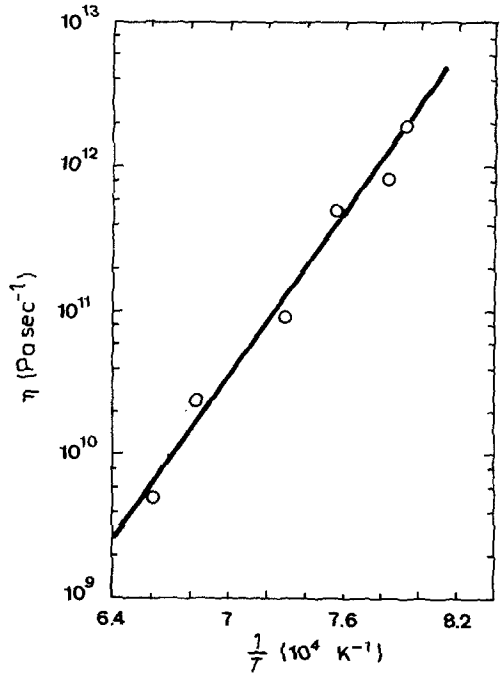

Figure 7 Temperature dependence of viscosity on the Arrhenius plot. Q = 82 kcal mol^{-1}.

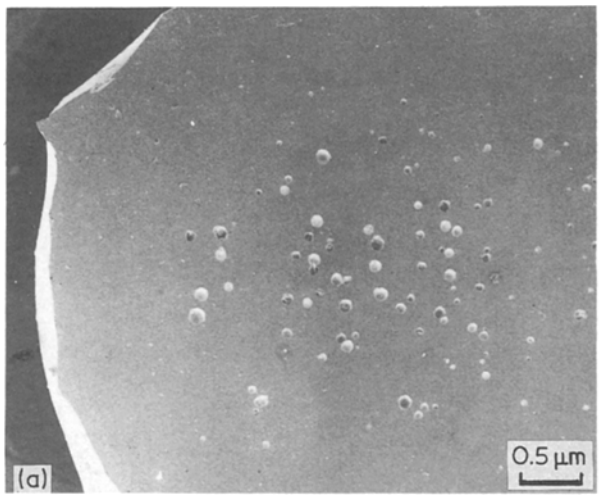

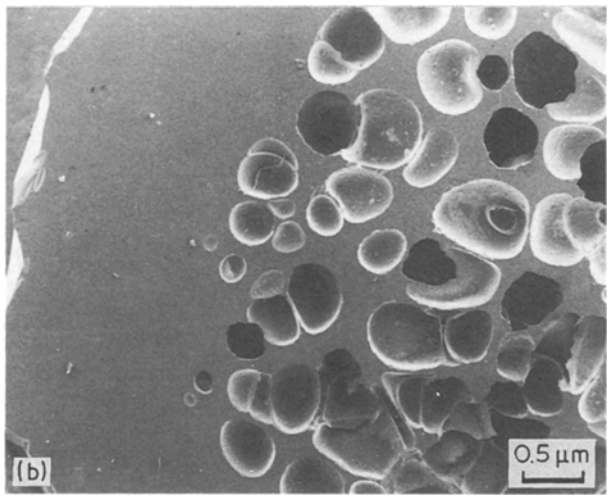

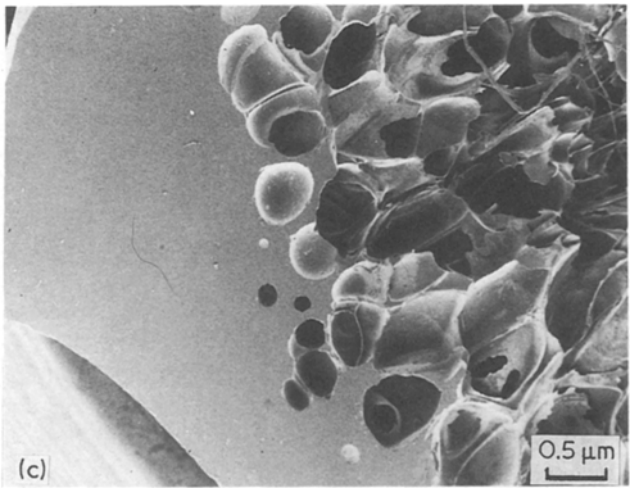

Figure 8 Scanning electron micrograph of sintered aerogel – foaming effect.

performed on the band situated at 2.73 μm show the hydroxyl content of our sample ranges between 3000 and 5000 p.p.m.

It is surprising that the sintering of material having such a complicated microstructure can be fitted with simple geometrical models. These results suggest that viscous sintering is relatively independent of the microstructure of the material as previously demonstrated [20]. Geometrical models can be used in so far as they account for the mean textural parameters (bulk density, mean pore size). The advantage of the cylinder model is that it is applicable over the whole range of relative density (up to 94%).

7. Foaming and crystallization

The material obtained after a controlled heat treatment above 1000° C is dense, transparent and exhibits physical properties similar to those of molten silica. However, if this material is heated at temperatures higher than 1200° C, undesirable phenomena, such as foaming and crystallization, occur. Scanning electron microscopy indicates that the foaming is initiated by the formation of spherical bubbles which appear first in the core of the material (Fig. 8a). Then the bubbles increase in size, and their shape is modified by the proximity of the neighbours (Fig. 8b). When the foaming proceeds, bubbles become interconnected forming a new closed porosity (Fig. 8c). Simultaneously with the foaming, the material crystallizes. The X-ray pattern is characteristic of the cristobalite form of SiO_2 [21].

Both phenomena, foaming and crystallization, are consequences of the high OH content present in the densified material. The infrared analysis exhibits a higher OH concentration at the centre of the sample (Fig. 9). During heat treatment, the "skin" of the sample is densified before the core, then the internal hydroxyl species included within the pores cannot be removed. These OH are transformed into H_2O vapour which migrates towards the centre of the material where it is trapped in the micropores. When the heat treatment proceeds at a higher temperature, the viscosity of the material decreases and the pressure of water inside the closed micropores increases leading to bloating.

8. Dehydration of the material

Several dehydration methods have been used to reduce the OH content. The dehydration treatment must be carried out before the closure of the pores of the material in such a way as to allow the internal OH to be removed. A common method is to increase the temperature slowly or to subject the material to a

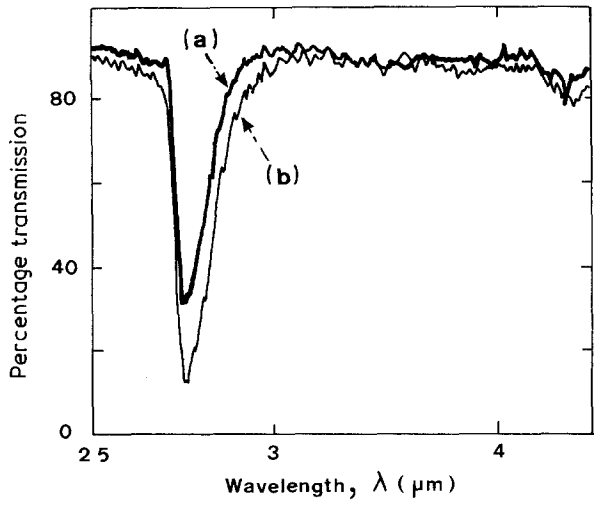

Figure 9 Infrared spectra of the sintered aerogel. (a) Periphery of the sample, (b) centre of the sample.

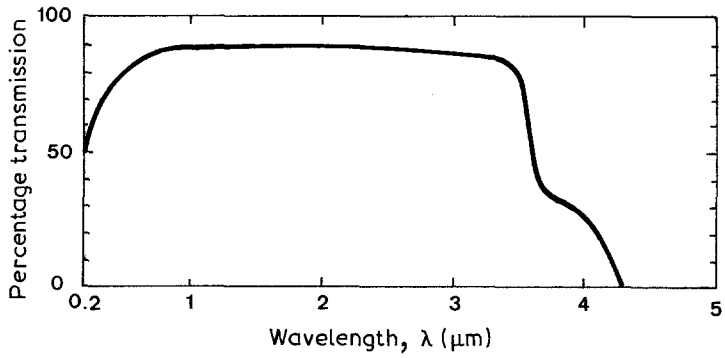

Figure 10 Optical transmission micrograph of the sintered aerogel in the wavelength range 0.2 to 5 μm.

preliminary isothermal heat treatment at a temperature lower than the densification temperature. This procedure produces glass having a residual OH content around 1200 p.p.m. If the material is densified under vacuum, the OH content can be as low as 600 p.p.m.

A good method by which to dehydrate the aerogels is to perform a chlorination treatment at 500° C using CCl_4 vapours mixed with an argon flux. The water content depends on the chlorination time. For times exceeding 2 h the residual water content is not detected (measured at 2.73 μm on 1 cm thick sample) and these silica glasses do not bloat or crystallize in the temperature range 1000 to 1500° C. As a consequence of the dehydration, the viscosity of the material increases [22] and thus the temperature at which the material easily densifies also increases (Table IV). It is worth noticing that this chlorination treatment is carried out at a very low temperature and for short durations. The sample is then heat treated under argon or helium gas to achieve the densification which occurs above 1350° C. Traces of oxygen in the gas and the high porosity of the aerogel are explanations offered to account for the fact that no chlorine reboil was observed at higher temperatures.

Figure 10 shows the ultraviolet, near infrared and infrared spectra of such a glass indicating undetectably low levels of transition metal impurities and OH content. Recently, this process has been extrapolated to multicomponent glasses SiO_2–B_2O_3 and SiO_2–P_2O_5 [23] or doped glasses with lanthanides [24].

9. The partially densified aerogel (P D A) – use of the aerogel porous structure as a host medium

The use of an open porosity of a glass to modify the nature of material has been previously applied to "Vycor" glass [25]. Xerogels are another matrix which allows nanocomposites [26], polymer glass composites [27], materials or dyes [28] and luminescence effect [29] to be obtained. However, the open porosity is well below that possible using aerogels.

In fact, a new kind of material has been developed in our laboratory from the aerogel–glass process. In this kind of material we use the totally open structure of the aerogel to allow migration of the liquid species throughout the whole volume of the gel. These liquid species may be, for example, salt in solution. Then, the liquid phase is eliminated, the porous composite (aerogel + salt) is fully densified giving rise to the synthesis of a multicomponent material. The porous structure of the aerogel is used as a volume host.

If we try to fill the aerogel with a liquid such as water, capillary phenomena (identical to those occurring during drying) induce the fracture of the gel. The capillary forces act on the three phases, liquid–solid–air, pulling or pushing apart neighbouring particles.

Due to the complexity of the aerogel texture, a detailed calculation of the local stresses during filling is difficult, but they are strongly dependent on the wetting angle, θ, the surface energy, γ, and the inverse of the pore size [30].

Thus, to avoid cracking during filling, two methods are proposed [31].

1. Use of a liquid having a low γ value which will diminish the magnitude of these forces.
2. Partial densification of the aerogel.

The heat treatment has two effects: it increases the mechanical strength of the material and removes the smallest pores so as to decrease the effects of the capillary phenomena.

A set of aerogels has been sintered to densities ranging from 0.3 to 1.2 and the materials were dipped in liquids having different γ values (Table V). During the time required for filling the gel (about 3 to 15 min depending on the liquid), cracks appear or the material remains monolithic (Fig. 11). With this diagram, a compromise can be found for the densification heat treatment. The final density must avoid the formation of cracks but it is necessary to retain a sufficiently large porosity to allow the migration of the liquids throughout the whole volume of the PDA material.

Table V gives the viscosity and the contact angles of the different liquids which are necessary parameters

TABLE IV OH content of the sintered aerogel as a function of the dehydration treatment

Dehydration treatment	OH content (p.p.m)	Densification temperature (°C)
Without	3500–5000	1150–1200
Isothermal treatment at 920° C	2600	1150–1200
Under vacuum	600	1200–1250
Chlorination treatment 2 h at 500° C	< 1	1300–1350

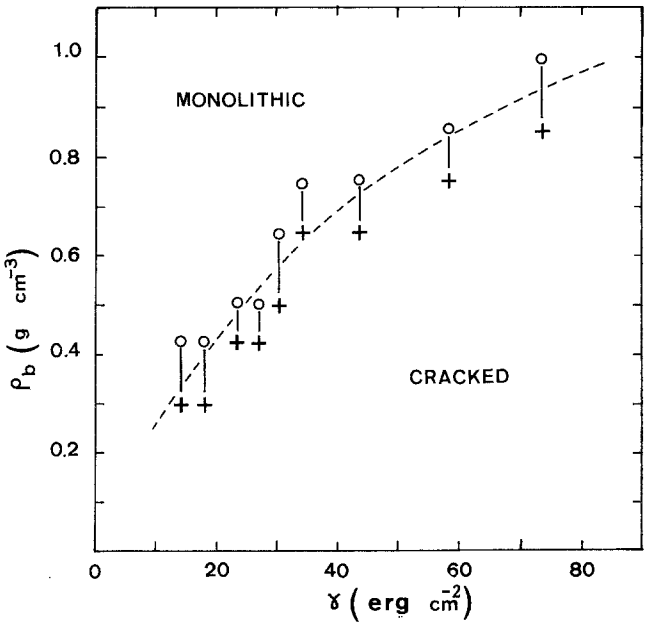

Figure 11 Diagram showing monolithic (○) or (+) cracked PDA as a function of the bulk density and the surface energy of liquids.

for the choice of the filling liquid. The θ values given in this table are the wetting angles measured on a flat surface of silica [32–34], the real contact angle can be different due to the roughness of the solid part of the surface [35]. The liquids often used are ethanol and water because of their properties (good solvents, wettability and low viscosities). Water is used for materials having a high density ($\rho_b > 1\,g\,cm^{-3}$) and ethanol when a large porosity is required (ρ_b in the range 0.5 to $1\,g\,cm^{-3}$). It must be pointed out that the diagram in Fig. 11 cannot be applied for materials which have not been densified, even when they have the required bulk density. For example, aerogels issued from a solution highly concentrated in TMOS or hydrolysed in acidic conditions have bulk densities in the range 0.4 to $0.5\,g\,cm^{-3}$ [3]. However, these materials crack during the filling by liquids even when the liquids have a low γ value (ethanol, threthylamine or isopentane). Xerogels with bulk density close to 0.8 to $1\,g\,cm^{-3}$ cannot be filled by ethanol without cracking. These results are explained by the fact that untreated materials (aerogels and xerogels) contain a small microporosity which weakens the solid part and which gives rise to capillary stresses larger than in the PDA material having the same bulk density. In those materials, ultramicropores are removed during the first stage of the sintering. Bulk density is a global evaluation of the pore volume but does not take into account the pore size distribution. The different steps of the PDA process are given in Fig. 12.

Liquids as different as salts in solution, monomers, gelifying solution or eletrolytes, can be used for the synthesis of various kinds of composite materials. To date, doped silica glasses (Dy III, Er III, Mn III, ...) have been investigated by migration of dissolved nitrates followed by a further densification [24]. Some of these glasses have been investigated for their magneto-optic properties [36]. The synthesis of gel–polymer, gel–gel, and gel–metal composites is in progress [37].

10. Conclusion

The synthesis of vitreous compounds from the sol–gel route has passed during the last decade from the field

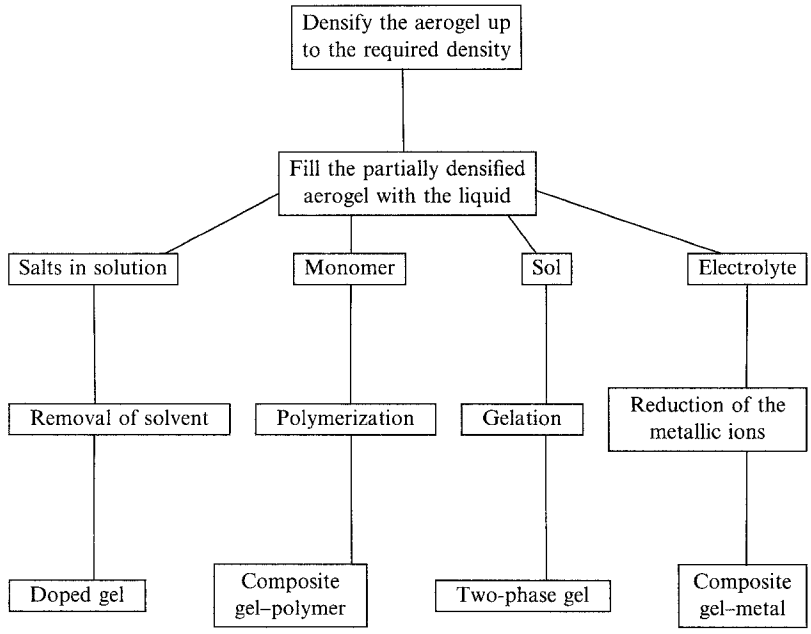

Figure 12 The PDA process.

TABLE V Surface energy, wetting angle and viscosity values of liquids useful for the PDA process

Liquid	Surface energy ($erg\,cm^{-2}$)	Wetting angle (deg)	Viscosity (cP)
Isopentan	13.7	–	0.22
Ethyl ether	17.1	–	0.23
Ethanol	22.3	0	1.2
Carbon tetrachloride	26.9	0 [32] 19 [33]	0.97
Benzene	28.9	28 [33]	0.65
Chlorobenzene	33.6	–	0.79
Aniline	42.9	82 [33]	4.4
Formamide	58.2	–	3.3
Water	72.06	7–10 [34] 40 [35]	1

of research technology. The major difficulty was obtaining bulk gels without cracks, which can be densified by a simple heat treatment. Several methods permitting control of the capillary phenomena which cause the cracking are now available and lead to monolithic material [38–41]. However, these procedures require long drying times and the results do not show a good reproducibility.

Hypercritical drying allows the rapid preparation of bulk monolithic aerogels with 100% certainty. These aerogels can be easily transformed into dense silica glass by means of heat treatments, such as oxidation, dehydration and densification. The dense amorphous material exhibits physical properties similar to those of the conventional silica glass with a high level of purity. Furthermore, the possibility of adjusting the pore volume of the aerogels and of using this porosity as a means to refil the material, extends the potentiality of the aerogel–glass process to a large range of products from doped silica glass to composites, as well as containers or dispersive media.

Acknowledgements

The authors are grateful for the financial support given by Corning Europe. They thank Rivista della Stazione Sperimentale del Vetro for allowing the publication of Figs 8, 9 and 10, and G. W. Scherer for many useful discussions of this work.

References

1. J. PHALIPPOU, T. WOIGNIER and M. PRASSAS, *J. Mater. Sci.* **25** (1990) 3111–3117.
2. R. VACHER, T. WOIGNIER, J. PHALIPPOU, J. PELOUS and E. COURTENS, *J. Non-Cryst. Solids* **106** (1988) 161.
3. T. WOIGNIER, J. PHALIPPOU and R. VACHER, *J. Mater. Res.* **4** (1989) 688.
4. T. WOIGNIER and J. PHALIPPOU, *Rev. Phys. Appl.* **C4** (1989) 179.
5. C. K. WU, *J. Non-Cryst. Solids* **41** (1980) 381.
6. R. F. BARTHOLOMEW, B. L. BUTLER, H. L. HOOVER and C. K. WU, *J. Amer. Ceram. Soc.* **63** (1980) 481.
7. P. VENKATESWARLU, *J. Chem. Phys.* **19** (1951) 298.
8. G. A. NICOLAON and S. J. TEICHNER, *Bull. Soc. Chim. France* **5** (1968) 1906.
9. R. VACHER, T. WOIGNIER, J. PELOUS and E. COURTENS, *Phys. Rev. B* **37** (1988) 6500.
10. T. WOIGNIER and J. PHALIPPOU, *J. Non-Cryst. Solids* **93** (1987) 17.
11. C. J. BRINKER and G. W. SCHERER, in "Ultrastructure Processing of Ceramics, Glasses and Composites", edited by L. L. Hench and D. R. Ulrich (Wiley, New York, 1984) p. 43.
12. A. F. CRAIEVICH, M. A. AEGERTER, D. I. DOS SANTOS, T. WOIGNIER and J. ZARZYCKI, *J. Non-Cryst. Solids* **86** (1986) 394.
13. T. LOURS, J. ZARZYCKI, A. CRAIEVICH, D. I. DOS SANTOS and M. AEGERTER, *ibid.* **95, 96** (1987) 1151.
14. S. K. MAITI, M. F. ASHBY and L. J. GIBSON, *Scripta Metall.* **18** (1984) 213.
15. D. STAUFFER, *J. Chem. Soc. Faraday Trans.* **72** (1972) 1354.
16. M. PRASSAS, J. PHALIPPOU and J. ZARZYCKI, in "Ultrastructure Processing of Ceramics, Glasses and Composites", edited by L. L. Hench and D. R. Ulrich (Wiley New York, 1986) p. 156.
17. J. FRENKEL, *J. Phys. (USSR)* **9** (1945) 385.
18. G. W. SCHERER, *J. Amer. Ceram. Soc.* **60** (1977) 237.
19. *Idem,* "Viscous Sintering of Inorganic Gels" in "Surface and Colloid Science", Vol. 14, edited by E. Matijewic (Plenum, New York, 1987) p. 265.
20. *Idem, J. Amer. Ceram. Soc.* **67** (1984) 709.
21. J. PHALIPPOU, T. WOIGNIER and J. ZARZYCKI, in "Ultrastructure Processing of Ceramics, Glasses and Composites", edited by L. L. Hench and D. R. Ulrich (Wiley, New York, 1984) p. 70.
22. G. HETHERINGTON, K. H. JACK and J. C. KENNEDY, *Phyus. Chem. Glasses* **5** (5) (1964) 130.
23. T. WOIGNIER and J. PHALIPPOU, Proceedings of the First Internation Workshop on Non-Crystalline Solids, edited by M. D. Baro and N. L. Clavaguera (World Scientific, Singapore, 1986) p. 415.
24. J. BOUAZIZ, T. WOIGNIER, D. BOURRET and R. SEMPERE, *J. Non-Cryst. Solids* **82** (1986) 225.
25. M. E. NORDBERG, *J. Amer. Ceram. Soc.* **27** (1944) 299.
26. D. HOFFMAN, R. ROY and S. KOMARNENI, *Mater. Lett.* **2** (1984) 245.
27. E. J. A. POPE and J. D. MACKENZIE, in "Better Ceramics through Chemistry II", Vol. 73 edited by C. J. Brinker, D. E. Clark and D. R. Ulrich (Materials Research Society, Pittsburgh, 1986) p. 809.
28. D. LEVY and D. AVNIR, *J. Phys. Chem.* **92** (1988) 4734.
29. B. DUNN, E. KNOBBE, J. M. KIERNAN, J. C. POUXVIEL and J. I. ZINK, in "Better Ceramics through Chemistry III", Vol. 121, edited by C. J. Brinker, D. E. Clark and D. R. Ulrich (Materials Research Society, Pittsburgh, 1988) p. 331.
30. M. PRASSAS, Thesis, Montpellier (1981).
31. T. WOIGNIER, Thesis, Montpellier (1984).
32. F. E. B. ARTELL and A. MERILL, *J. Phys. Chem.* **36** (1932) 1178.
33. F. E. BARTELL and H. J. OSTERHOF, *ibid.* **37** (1933) 543.
34. L. HOLLAND," The Properties of Glass Surfaces", (Chapman and Hall, London, 1964) p. 359.
35. J. J. HITCHCOCK, N. T. CARROLL and M. G. NICHOLAS, *J. Mater. Sci.* **16** (1981) 714.
36. J. BOUAZIZ, D. BOURRET, R. SEMPERE and J. REGNIER, *J. Non-Cryst. Solids* **82** (1986) 183.
37. D. BOURRET, R. SEMPERE, A. SIVADE and J. BOUAZIZ, *Rev. Phys. Appl.* **C4** (1989) 71.
38. E. M. RABINOVICH, D. W. JOHNSON, J. B. MacCHESNEY and E. M. VOGEL, *J. Amer. Ceram. Soc.* **66** (1983) 683.
39. G. W. SCHERER and J. C. LUONG, *J. Non-Cryst. Solids* **63** (1984) 163.
40. G. ORCEL and L. L. HENCH, Proceedings of the 8th Annual Conference on Composites and Advanced Ceramic Materials, Cocoa Beach (The Amer. Ceram. Soc. 1984) p. 15.
41. M. TOKI, S. MIYASHITA, T. TAKEUCHI, S. KANABE and A. KOCHI, *J. Non-Cryst. Solids* **100** (1988) 479.

Received 7 February
and accepted 7 June 1989